

Millimeter and submillimeter wave spectra of ^{13}C -glycolaldehydes^{*}

I. Haykal, R. A. Motiyenko, L. Margulès, and T. R. Huet

Laboratoire de Physique des Lasers, Atomes et Molécules, Bâtiment P5, CNRS, UMR 8523, Université Lille 1,
59655 Villeneuve d'Ascq Cedex, France
e-mail: Therese.Huet@univ-lille1.fr

Received 25 October 2012 / Accepted 9 November 2012

ABSTRACT

Context. Glycolaldehyde (CH_2OHCHO) is the simplest sugar and an important intermediate in the path toward forming more complex biologically relevant molecules. Astronomical surveys of interstellar molecules, such as those available with the very sensitive ALMA telescope, require preliminary laboratory investigations of the microwave and submillimeter-wave spectra of molecular species including new isotopologs – to identify these in the interstellar media.

Aims. To achieve the detection of the ^{13}C isotopologs of glycolaldehyde in the interstellar medium, their rotational spectra in the millimeter and submillimeter-wave regions were studied.

Methods. The spectra of $^{13}\text{CH}_2\text{OHCHO}$ and $\text{CH}_2\text{OH}^{13}\text{CHO}$ were recorded in the 150–945 GHz spectral range in the laboratory using a solid-state submillimeter-wave spectrometer in Lille. The observed line frequencies were measured with an accuracy of 30 kHz up to 700 GHz and of 50 kHz above 700 GHz. We analyzed the spectra with a standard Watson Hamiltonian.

Results. About 10 000 new lines were identified for each isotopolog. The spectroscopic parameters were determined for the ground- and the three lowest vibrational states up to 945 and 630 GHz. Previous microwave assignments of $^{13}\text{CH}_2\text{OHCHO}$ were not confirmed.

Conclusions. The provided line-lists and sets of molecular parameters meet the needs for a first astrophysical search of ^{13}C -glycolaldehydes.

Key words. ISM: molecules – submillimeter: ISM – methods: laboratory – line: identification

1. Introduction

Glycolaldehyde (Fig. 1), the smallest sugar, is considered as a probable prebiotic molecule since its first detection in the interstellar medium (ISM) by (Hollis et al. 2000). In a recent paper (Jørgensen et al. 2012) the first detection of 13 transitions of glycolaldehyde around a solar-type young star was presented, which were made with the Atacama Large Millimeter Array (ALMA) observations of the Class 0 protostellar binary IRAS 16293-2422 at 220 GHz (six transitions) and 690 GHz (seven transitions). The order of magnitude increase in line density in these early ALMA data illustrates its huge potential to reveal the full chemical complexity associated with the formation of solar system analogs. Especially the constraints on the chemical formation of glycolaldehyde and other organic species have been discussed. According to Jørgensen et al. (2012), the relative abundances appear to be consistent with UV photochemistry of a $\text{CH}_3\text{OH} - \text{CO}$ mixed ice that has undergone mild heating. This conclusion is consistent with previous published results (Bennett & Kaiser 2007) even if possible gas-phase pathways have also been proposed (Jalbout et al. 2007) and discussed (Simakov et al. 2011). In their article, Bennett & Kaiser (2007) paid special attention to the investigation of the glycolaldehyde formation process and its isomers (methyl formate and acetic acid), which obey the same empirical formula $\text{C}_2\text{H}_4\text{O}_2$. Their relative abundance, for example, was reported by Hollis et al. (2001) to be 52:2:1 (methyl formate:acetic acid:glycolaldehyde) in Sgr B2.

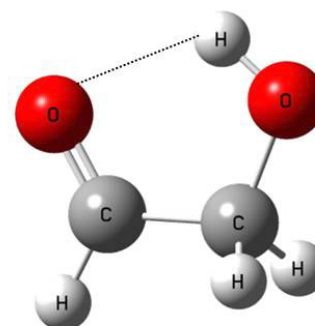


Fig. 1. Schematic view of the most stable conformer of glycolaldehyde, stabilized by a weak hydrogen bond $\text{OH} \cdots \text{O}=\text{C}$ binding the two functional groups.

In addition to the ability of this hydroxyaldehyde diose to become involved in the production of important biomolecules (glycolaldehyde phosphates, amino acids, etc), the ^{13}C isotopologs of glycolaldehyde are of special importance to astrophysicists. Detecting them in the future will enable us to measure the abundance ratio of ^{12}C over ^{13}C isotopes by measuring the ratio of the abundance of their respective isotopomers. Observing isotopic abundances in the interstellar medium provides an avenue for quantitatively assessing stellar nucleosynthesis and therefore Galactic chemical evolution. The $^{12}\text{C}/^{13}\text{C}$ isotope ratio is also considered an important tracer because it reflects the relative degree of primary to secondary processing in stars (Milam et al. 2005).

The present study investigates the rotational structure of the ground states and the three lowest vibrational modes for the

* Full Tables 3 and 4 are only available at the CDS via anonymous ftp to cdsarc.u-strasbg.fr (130.79.128.5) or via <http://cdsarc.u-strasbg.fr/viz-bin/qcat?J/A+A/549/A96>

two ^{13}C isotopomers of glycolaldehyde. Although they are so important on the astrophysical scale, the two ^{13}C -isotopologs of glycolaldehyde, $^{13}\text{CH}_2\text{OHCHO}$ and $\text{CH}_2\text{OH}^{13}\text{CHO}$, were studied only once in the past 40 years. Indeed, [Marstokk & Møllendal \(1973\)](#) reported the analysis of spectra recorded in the microwave range (12.4–36.3 GHz) with a spectral accuracy of 0.25 MHz. Ten and eighteen lines were observed in natural abundance and were identified to be $^{13}\text{CH}_2\text{OHCHO}$ and $\text{CH}_2\text{OH}^{13}\text{CHO}$, respectively. The data were fitted to a standard Watson Hamiltonian, providing a set of molecular parameters including the principal rotational constants and the quartic centrifugal distortion parameters. [Marstokk & Møllendal \(1973\)](#) also re-measured the permanent dipole moment of the parent species: $\mu_a = 0.2620 \pm 0.002$ D, $\mu_b = 2.330 \pm 0.01$ D, and $\mu_{\text{tot}} = 2.340 \pm 0.01$ D. Glycolaldehyde is a fairly light molecule ($M = 60$) whose typical μ_b type spectra have their maximum absorption at 820 GHz (at 300 K) and extend far beyond 1 THz. If glycolaldehyde and its isotopic species are interesting objects for highly sensitive terahertz radio telescopes such as ALMA or Herschel, the results of [Marstokk & Møllendal \(1973\)](#) are insufficient to provide reliable frequency predictions in the terahertz range. Moreover, as we show below, the previous assignment of one of the ^{13}C species is most probably erroneous and could not be used for astrophysical observations. The deuterated isotopologs of glycolaldehyde have recently been studied in the millimeter-wave region (150–630 GHz) by [Bouchez et al. \(2012\)](#). This spectroscopic study was motivated by a future comparison of the D/H ratios for better understanding the formation of glycolaldehyde in hot cores and hot corinos. According to the relative abundance of the $^{13}\text{C}/^{12}\text{C}$ and D/H ratios observed in the ISM, it is probably useful to be able to also identify in the future the two ^{13}C -isotopologs of glycolaldehyde in the future. To this end we studied the spectroscopy of $^{13}\text{CH}_2\text{OHCHO}$ and $\text{CH}_2\text{OH}^{13}\text{CHO}$ in the laboratory in the millimeter-wave and submillimeter-wave ranges. Precise molecular parameters were obtained for the ground and first three excited vibrational states of the two species, providing a line-list for a future detection, with an absolute frequency accuracy better than 30 kHz in the spectral ranges covered by the ALMA and Herschel telescopes.

2. Experiment

The millimeter- and submillimeter-wave spectra of ^{13}C -glycolaldehydes were recorded using the Lille spectrometer based on solid-state sources. The frequency source is a 20 GHz synthesizer (Agilent, model E8257D) that is stabilized on a global positioning system. The output frequency (12.5–18.4 GHz) is multiplied by six and amplified by an active sextupler (Spacek), providing an output power of +15 dBm in the W-band range (75–110 GHz). Passive Schottky multipliers ($\times 2$, $\times 3$, $\times 5$, $\times 3 \times 2$, $\times 3 \times 3$, Virginia Diodes Inc.) are used in the last stage of the frequency multiplication chain to provide a useful signal in the 150–990 GHz spectral range. The commercial samples of $^{13}\text{CH}_2\text{OHCHO}$ and $\text{CH}_2\text{OH}^{13}\text{CHO}$ (Omicron Biochemicals, Inc., 99% purity, in aqueous solution) were dehydrated and used without additional purification. It was found later that the two dehydrated commercial samples contained a mixture of the two ^{13}C -glycolaldehydes in a ratio equal to $^{13}\text{CHO}/^{13}\text{CH}_2\text{O} = 0.59$ and $^{13}\text{CH}_2\text{O}/^{13}\text{CHO} = 0.67$, but without impurity. The absorption cell is a stainless-steel tube (6 cm diameter, 220 cm long). The sample pressure was equal to 20×10^{-6} bars, and slightly increased up to 40×10^{-6} bars in the 700–945 GHz region. To improve the signal sensitivity, the sources were frequency modulated at 10 kHz and lock-in

detection with the second harmonic was used. Absorption signals were detected by an InSb liquid He-cooled bolometer (QMC Instruments Ltd.) and processed on a computer. Spectra of the two samples were recorded at room temperature ($T = 294$ K) in the 150–215, 230–315, 400–530, 500–630, and 700–945 GHz regions with a frequency step of 30, 36, 48, 54, and 76 kHz and with an acquisition time of 35 ms. The line frequencies were obtained by adjusting the second derivative of a Gaussian profile on the observed signals, knowing that the linewidths are limited by Doppler broadening (around 1 MHz at 600 GHz). The absolute accuracy of the line-center frequency is estimated to be better than 30 kHz (50 kHz above 700 GHz) for isolated lines, and can be as high as 100 kHz (150 kHz above 700 GHz) for blended or very weak lines.

3. Analysis

At first, the strongest lines associated with the ground state were considered for both $^{13}\text{CH}_2\text{OHCHO}$ and $\text{CH}_2\text{OH}^{13}\text{CHO}$. In previous spectroscopic works as well as in the present one, a standard asymmetric-top Hamiltonian with a Watson A-reduction in the I' -representation was employed. Consequently, the rotational structure is characterized by the $J_{K_a K_c}$ quantum numbers. The spectral data were fitted by means of the ASFIT¹ and ASROT¹ suite of programs. Final results are available at the CDS, using the formats of the program suite SPFIT and SPCAT ([Pickett 1991](#)), which are commonly used by astrophysicists ([Pearson et al. 2010](#)).

At the initial stage of the line assignment, we used predictions based on the principal rotational constants from [Marstokk and Møllendal \(1973\)](#) while the value of the quartic and sextic distortion parameters were fixed to the corresponding values of the CH_2OHCHO parent molecule ([Widicus Weaver et al. 2005](#)). We first searched for the intense R-branch lines of the low K_a quantum number ($K_a = 0, 1$) with respect to the selection rule associated with the μ_b type transitions ($\Delta K_a = \pm 1$, $\Delta K_c = \pm 1$). Their doublet structure helped us to recognize them, cf. [Fig. 2](#). Following the systematic decrease of the splitting within the doublets and the increase of the line intensity with the increase of the J quantum number, we collected doublets up to $J = 21$ for $\text{CH}_2\text{OH}^{13}\text{CHO}$ and $J = 20$ for $^{13}\text{CH}_2\text{OHCHO}$ in the 150–215 GHz frequency range. Meanwhile, the observed minus calculated frequency shift increased quickly, reaching 5.5 MHz at $J = 21$ for $\text{CH}_2\text{OH}^{13}\text{CHO}$ and 43 MHz at $J = 20$ for $^{13}\text{CH}_2\text{OHCHO}$. Consequently, the new millimeter-wave lines of each isotopomer were fitted together with the microwave lines measured by [Marstokk and Møllendal \(1973\)](#). The initial set of parameters was refined and new and more accurate predictions were generated. However, we had to exclude four microwave lines from the fit for $\text{CH}_2\text{OH}^{13}\text{CHO}$ because their observed-calculated residuals did not satisfy the 3σ criteria (where σ is the experimental measurement uncertainty). We found that the A rotational constant obtained by [Marstokk and Møllendal \(1973\)](#) for $^{13}\text{CH}_2\text{OHCHO}$ ([Marstokk & Møllendal 1973](#)) could not be associated with the ground state. Therefore all microwave transitions ([Marstokk & Møllendal 1973](#)) were omitted from our analysis. The next step was to proceed with the assignment by increasing the K_a quantum number. In this frequency range $K'_{a\text{MAX}} = 22$ for $J'_{\text{MAX}} = 62$ ($\text{CH}_2\text{OH}^{13}\text{CHO}$) and $K'_{a\text{MAX}} = 25$ for $J'_{\text{MAX}} = 67$ ($^{13}\text{CH}_2\text{OHCHO}$) were reached. Afterward, we searched for the

¹ Kisiel (2012), programs are available on the <http://www.ifpan.edu.pl/~kisiel/asym/asym.htm#asfit>

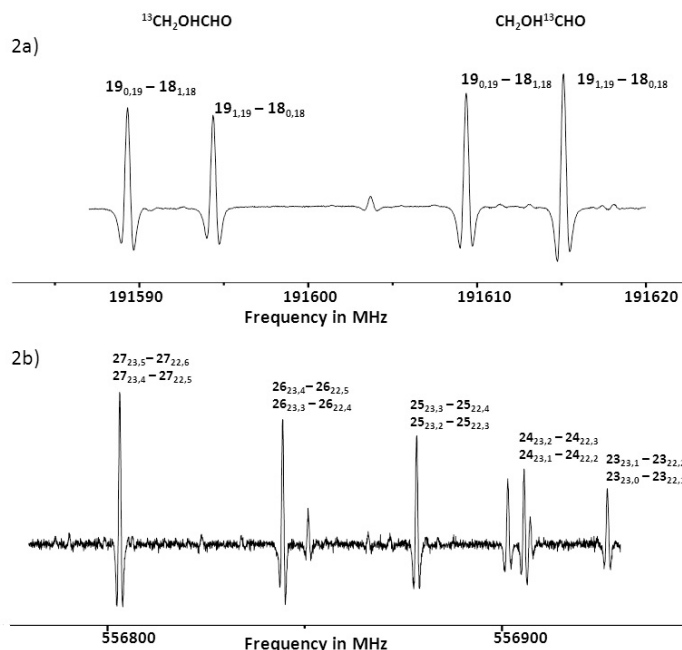


Fig. 2. a) Strong R-line doublets associated with $K_a = 0, 1$, observed in the 191 GHz range with a sample containing the two ^{13}C -glycolaldehydes and b) weak Q-lines of $^{13}\text{CH}_2\text{OHCHO}$ associated with $K_a = 22$, observed in the 557 GHz range. All signals are assigned to the ground states and are labeled $(J_{K_a K_c})' \leftarrow (J_{K_a K_c})''$.

Q type transitions and gathered them up to $J', K_a' = 64, 14$ ($\text{CH}_2\text{OH}^{13}\text{CHO}$) and $J', K_a' = 66, 15$ ($^{13}\text{CH}_2\text{OHCHO}$), cf. Fig. 2. Pursuing the analysis up to 950 GHz, we assigned R and Q transitions up to $K_a' = 37$ and $J' = 93$ following the same strategy. At the end the weak lines associated with the μ_a type of transitions ($\Delta K_a = 0, \Delta K_c = \pm 1$) were assigned. We finally determined a set of 20 molecular parameters for each molecule, including centrifugal distortion parameters up to the octic terms, by fitting a total of 4218 assigned lines for $\text{CH}_2\text{OH}^{13}\text{CHO}$ and 4655 for $^{13}\text{CH}_2\text{OHCHO}$, with a relevant root mean square deviation (rms) of 31 and 29 kHz. The final sets of molecular parameters are presented in Tables 1 and 2. The number of assigned lines and the maximal values of the observed quantum numbers are also given. The good quality of the spectra provided by our spectrometer and the high signal-to-noise ratio allowed us to proceed with assigning of the rotational structure of the three lowest excited vibrational modes (Fig. 3). The calculated vibrational energies for the parent molecule are approximately 213 cm^{-1} (ν_1 , the C–C torsion mode), 294 cm^{-1} (ν_2 , the C–C–O bending mode), and 426 cm^{-1} (ν_3 , the O–H torsion mode) (Senent 2004). To start the analysis of $\nu_1 = 1$, the rotational constants were roughly predicted using the vibration-rotation constants α of the parent molecule ($\beta = A, B, C$) (Widicus Weaver et al. 2005):

$$\alpha_{\tau}^{\beta} = \beta(v_{\tau} = 0) - \beta(v_{\tau} = 1).$$

This relation also served to predict the first set of rotational constants for $\nu_2 = 1$ and $\nu_3 = 1$. At the beginning of the analysis, the quartic, sextic, and octic distortion parameters values were fixed to those of the ground state (see Tables 1 and 2). This first set of parameters supplied the preliminary predictions. Taking into account the decrease of the Boltzmann distribution and following the same assignment strategy as for the ground state, we could assign the rotational structure up to 630 GHz. The rotational constants and the centrifugal distortion parameters up to the sextic terms were determined for the three lowest excited

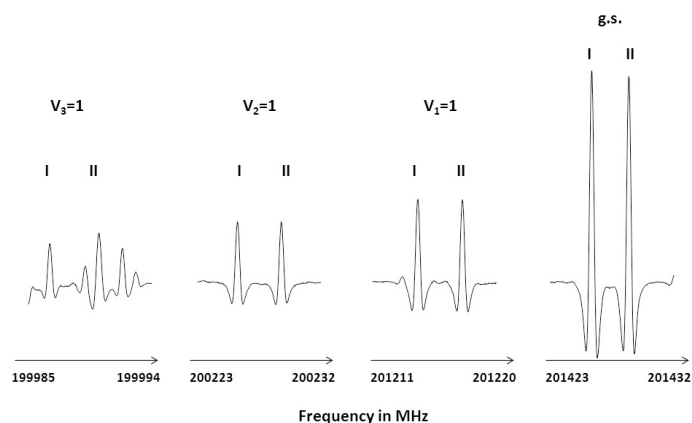


Fig. 3. Example of strong lines of $^{13}\text{CH}_2\text{OHCHO}$, i.e. $J_{K_a K_c} = 20_{0,20} - 19_{1,19}$ (I) and $J_{K_a K_c} = 20_{1,20} - 19_{0,19}$ (II), observed simultaneously in the ground state and in the first three excited vibrational states in the 200 GHz range at 294 K.

modes of the two isotopomers. They are presented in Tables 1 and 2, for $\text{CH}_2\text{OH}^{13}\text{CHO}$ and $^{13}\text{CH}_2\text{OHCHO}$. Finally, a full list of assigned lines is given in Tables 3 and 4 for $\text{CH}_2\text{OH}^{13}\text{CHO}$ and $^{13}\text{CH}_2\text{OHCHO}$. The tables contain the rotational assignments, the vibrational assignment, the observed frequencies, the observed-calculated frequency residuals, and the experimental uncertainties.

The tabulated values for the ^{13}C -glycolaldehydes partition function are given in Table 5, with $Q(T)_{\text{tot}} = Q(T)_{\text{vib}} Q(T)_{\text{rot}}$. Various temperatures are considered. $Q(T)_{\text{rot}}$ was calculated as

$$Q(T)_{\text{rot}} = \sqrt{\frac{\pi}{ABC} \left(\frac{kT}{h} \right)^3},$$

where A, B , and C represent the rotational constants of the ground state in MHz. As noted by Widicus Weaver et al. (2005), the glycolaldehyde partition function increases significantly when taking into account the vibrational contribution. This is mainly because of the low-frequency vibrational modes. Unfortunately, no experimental or theoretical data are available for the ^{13}C -glycolaldehydes. Meanwhile, regarding the weak differences in atomic and molecular masses (one ^{12}C atom is replaced by one ^{13}C atom and $M_{\text{tot}} = 61$ instead of $M_{\text{tot}} = 60$), we estimated the vibrational partition function using the observed or calculated frequencies for the main species. The three lowest calculated frequencies (ν_1, ν_2, ν_3) were taken from Senent (2004), the observed band centers ($\nu_5, \nu_6, \nu_8, \nu_{10} - \nu_{18}$) in the infrared region were taken from Jetzki et al. (2004) and the others (ν_4, ν_7, ν_9) from Carbonniere & Pouchan (2012). Indeed, these last authors performed a high-level ab initio calculation limited to the mid-infrared region. Their results agree well with the few experimental data (Jetzki et al. 2004). Putting the zero energy at the ground state level, the vibrational partition function was calculated using the expression

$$Q(T)_{\text{vib}} = \prod_{i=1}^{3N-6} \frac{1}{1 - e^{-E_i/kT}}.$$

4. Conclusions

The rotational structure of the two ^{13}C -isotopologs of glycolaldehyde was characterized in the laboratory for the ground

Table 1. Determined parameters for the ground state and first lowest excited modes of CH₂OH¹³CHO.

Parameter	g.s.	$\nu_1 = 1$	$\nu_2 = 1$	$\nu_3 = 1$
A/MHz	18 259.420856(138)	18 276.114890(202)	18 389.804481(207)	18 339.529892(210)
B/MHz	6472.436365(46)	6429.762469(73)	6424.945607(103)	6392.817976(96)
C/MHz	4924.607952(39)	4920.695284(68)	4894.384811(77)	4889.456137(79)
Δ_J /kHz	6.0549035(175)	6.109038(42)	6.025532(66)	6.195241(59)
Δ_{JK} /kHz	-20.074050(144)	-19.706090(265)	-21.22054(32)	-22.859886(298)
Δ_K /kHz	47.14390(34)	47.73743(55)	51.24159(52)	52.62572(56)
δ_J /kHz	1.7923852(60)	1.7928296(138)	1.8035355(281)	1.8204557(221)
δ_K /kHz	8.594098(171)	7.414565(295)	10.48764(49)	8.68613(42)
Φ_J /Hz	-0.00672850(261)	-0.006.6487(82)	-0.0085328(189)	-0.0028636(150)
Φ_{JK} /Hz	0.165951(41)	0.093486(187)	0.22492(32)	0.176211(259)
Φ_{KJ} /Hz	-0.792121(172)	-0.58880(63)	-1.09705(102)	-0.80421(89)
Φ_K /Hz	1.06114(42)	0.95730(69)	1.37584(90)	1.16269(86)
ϕ_J /Hz	-0.00209800(116)	-0.0018600(35)	-0.0033456(93)	-0.0003544(68)
ϕ_{JK} /Hz	-0.020704(70)	0.007253(110)	-0.070693(256)	-0.011349(209)
ϕ_K /Hz	0.26838(50)	-0.39595(192)	0.8892(32)	0.28761(286)
L_{JK} /mHz	-0.0046785(260)	(a)	(a)	(a)
L_{KKJ} /mHz	0.022324(74)	(a)	(a)	(a)
L_K /mHz	-0.028327(177)	(a)	(a)	(a)
l_{JK} /mHz	-0.0005629(72)	(a)	(a)	(a)
l_{KJ} /mHz	0.001660(101)	(a)	(a)	(a)
J_{MAX}, K_{aMAX}	93, 37	62, 25	63, 25	64, 25
Freq _{MAX} /GHz	945	630	630	630
Nb lines	4218	1982	1629	1571
Fit rms/kHz	31	27	25	26

Notes. The uncertainties (one standard deviation) are reported between parentheses. ^(a) Fixed to the corresponding value of the ground state.

Table 2. Determined parameters for the ground state and first lowest excited modes of ¹³CH₂OHCHO.

Parameter	g.s.	$\nu_1 = 1$	$\nu_2 = 1$	$\nu_3 = 1$
A/MHz	18 142.347585(137)	18 158.665788(189)	18 271.186559(194)	18 220.212215(189)
B/MHz	6486.371688(42)	6443.512178(68)	6439.195622(82)	6407.190316(87)
C/MHz	4924.025217(38)	4920.138890(64)	4893.909288(70)	4889.259376(73)
Δ_J /kHz	6.0421246(160)	6.097184(40)	6.013999(53)	6.184484(49)
Δ_{JK} /kHz	-19.380210(145)	-18.993301(247)	-20.566390(242)	-22.150861(233)
Δ_K /kHz	46.29710(35)	46.87797(51)	50.43534(50)	51.70740(52)
δ_J /kHz	1.7971024(49)	1.7981212(141)	1.8087097(176)	1.8270081(195)
δ_K /kHz	8.739649(166)	7.562799(303)	10.64113(35)	8.83449(43)
Φ_J /Hz	-0.00680317(217)	-0.0067594(82)	-0.0087018(117)	-0.002.8859(105)
Φ_{JK} /Hz	0.164691(42)	0.090129(219)	0.225627(234)	0.17676(33)
Φ_{KJ} /Hz	-0.776215(181)	-0.56439(72)	-1.08403(82)	-0.79714(115)
Φ_K /Hz	1.03579(46)	0.92577(70)	1.35118(78)	1.13950(97)
ϕ_J /Hz	-0.00216263(90)	-0.0019296(35)	-0.0034482(50)	-0.0003940(50)
ϕ_{JK} /Hz	-0.021306(70)	0.006333(134)	-0.071921(150)	-0.009.972(156)
ϕ_K /Hz	0.27266(44)	-0.39518(217)	0.89508(262)	0.3040(37)
L_{JK} /mHz	-0.004671(34)	(a)	(a)	(a)
L_{KKJ} /mHz	0.022005(72)	(a)	(a)	(a)
L_K /mHz	-0.027932(191)	(a)	(a)	(a)
l_{JK} /mHz	-0.0005147(75)	(a)	(a)	(a)
l_{KJ} /mHz	0.002144(85)	(a)	(a)	(a)
J_{MAX}, K_{aMAX}	93, 37	62, 25	63, 25	64, 25
Freq _{MAX} /GHz	945	630	630	630
Nb lines	4655	2204	1884	1779
Fit rms/kHz	29	22	23	23

Notes. The uncertainties (one standard deviation) are reported between parentheses. ^(a) Fixed to the corresponding value of the ground state.

Table 3. List of the assigned lines for the rotation spectrum of $\text{CH}_2\text{OH}^{13}\text{CHO}$ in the ground state and the three first excited vibrational states ($\nu_1 = 1, \nu_2 = 1, \nu_3 = 1$).

State	J'	K'_a	K'_c	J''	K''_a	K''_c	Frequency (MHz)	Obs-Calc. (MHz)	Uncertainty (MHz)	Intensity weighting for blended lines
g.s.	20	17	4	20	16	5	412885.509	0.00708	0.030	5.00E-01
g.s.	20	17	3	20	16	4	412885.509	0.00708	0.030	5.00E-01
g.s.	21	17	5	21	16	6	412812.621	-0.01769	0.030	5.00E-01
g.s.	21	17	4	21	16	5	412812.621	-0.01769	0.030	5.00E-01
...
...
$\nu_1 = 1$	20	17	4	20	16	5	414244.956	0.00293	0.030	5.00E-01
$\nu_1 = 1$	20	17	3	20	16	4	414244.956	0.00293	0.030	5.00E-01
$\nu_1 = 1$	21	17	5	21	16	6	414177.132	0.02522	0.030	5.00E-01
$\nu_1 = 1$	21	17	4	21	16	5	414177.132	0.02522	0.030	5.00E-01
...
...
$\nu_2 = 1$	20	17	4	20	16	5	418450.873	-0.00046	0.030	5.00E-01
$\nu_2 = 1$	20	17	3	20	16	4	418450.873	-0.00046	0.030	5.00E-01
$\nu_2 = 1$	21	17	5	21	16	6	418382.619	0.01600	0.030	5.00E-01
$\nu_2 = 1$	21	17	4	21	16	5	418382.619	0.01600	0.030	5.00E-01
...
...
$\nu_3 = 1$	20	17	4	20	16	5	417434.648	0.03930	0.030	5.00E-01
$\nu_3 = 1$	20	17	3	20	16	4	417434.648	0.03930	0.030	5.00E-01
$\nu_3 = 1$	21	17	5	21	16	6	417372.346	0.00343	0.030	5.00E-01
$\nu_3 = 1$	21	17	4	21	16	5	417372.346	0.00343	0.030	5.00E-01
...
...

Notes. The complete table is available at the CDS.

Table 4. List of the assigned lines for the rotation spectrum of $^{13}\text{CH}_2\text{OHCHO}$ in the ground state and the three first excited vibrational states ($\nu_1 = 1, \nu_2 = 1, \nu_3 = 1$).

State	J'	K'_a	K'_c	J''	K''_a	K''_c	Frequency (MHz)	Obs-Calc. (MHz)	Uncertainty (MHz)	Intensity weighting for blended lines
g.s.	20	17	4	20	16	5	408 776.594	0.01085	0.030	5.00E-01
g.s.	20	17	3	20	16	4	408 776.594	0.01085	0.030	5.00E-01
g.s.	21	17	5	21	16	6	408 699.835	0.01356	0.030	5.00E-01
g.s.	21	17	4	21	16	5	408 699.835	0.01356	0.030	5.00E-01
...
...
$\nu_1 = 1$	20	17	4	20	16	5	410 127.655	0.00671	0.030	5.00E-01
$\nu_1 = 1$	20	17	3	20	16	4	410 127.655	0.00671	0.030	5.00E-01
$\nu_1 = 1$	21	17	5	21	16	6	410 056.011	-0.00882	0.030	5.00E-01
$\nu_1 = 1$	21	17	4	21	16	5	410 056.011	-0.00882	0.030	5.00E-01
...
...
$\nu_2 = 1$	20	17	4	20	16	5	414 284.402	-0.02642	0.030	5.00E-01
$\nu_2 = 1$	20	17	3	20	16	4	414 284.402	-0.02642	0.030	5.00E-01
$\nu_2 = 1$	21	17	5	21	16	6	414 212.368	0.00509	0.030	5.00E-01
$\nu_2 = 1$	21	17	4	21	16	5	414 212.368	0.00509	0.030	5.00E-01
...
...
$\nu_3 = 1$	20	17	4	20	16	5	413 240.435	0.01363	0.030	5.00E-01
$\nu_3 = 1$	20	17	3	20	16	4	413 240.435	0.01363	0.030	5.00E-01
$\nu_3 = 1$	21	17	5	21	16	6	413 174.371	0.00898	0.030	5.00E-01
$\nu_3 = 1$	21	17	4	21	16	5	413 174.371	0.00898	0.030	5.00E-01
...
...

Notes. The complete table is available at the CDS.

state and the first three excited vibrational modes up to 945 and 630 GHz. High-quality spectra were continuously recorded with an absolute frequency accuracy better than 30 kHz. The sets of molecular parameters we determined can be used to generate

predictions in the range of one to several hundred GHz at the experimental accuracy, without bias. These isotopologs of glycolaldehyde are relevant targets for the ALMA interferometers owing to their high sensitivity and spatial resolution.

Table 5. Rotational and vibrational partition functions at various temperatures for the ^{13}C isotopomers of glycolaldehyde ($\text{CH}_2\text{OH}^{13}\text{CHO}$ and $^{13}\text{CH}_2\text{OHCHO}$) and for their parent molecule. $Q(T)_{\text{tot}} = Q(T)_{\text{vib}} Q(T)_{\text{rot}}$.

	$\text{CH}_2\text{OH } ^{13}\text{CHO}$	$^{13}\text{CH}_2\text{OHCHO}$	CH_2OHCHO
Temperature (K)	$Q(T)_{\text{rot}}$	$Q(T)_{\text{rot}}$	$Q(T)_{\text{vib}}$
300	36 355.02	36 435.08	2.612
200	19 789.16	19 832.75	1.542
150	12 853.44	12 881.75	1.245
50	2473.65	2479.10	1.002
10	221.25	221.74	1.000

Acknowledgements. The authors gratefully acknowledge Jean-Claude Guillemin (Ecole Nationale Supérieure de Chimie de Rennes, France) for his help in conditioning the samples. This work was supported by the French ANR agency under contract ANR-08-BLAN-0054, by the French CNRS-INSU programme “Action sur Projet Physico-Chimie du Milieu Interstellaire” and by the Centre National d’Etudes Spatiales (CNES).

References

- Bennett, C. J., & Kaiser, R. I. 2007, ApJ, 661, 899
 Bouchez, A., Margulès, L., Motiyenko, R. A., et al. 2012, A&A, 540, A51
 Carbonniere, P., & Pouchan, P. 2012, Theor. Chem. Acc., 131, 1183
 Hollis, J. M., Lovas, F. J., & Jewell, P. R. 2000, ApJ, 540, 107
 Hollis, J. M., Vogel, S. N., Snyder, L. E., et al. 2001, ApJ, 554, 81
 Jalbout, A. F., Abrell, L., Adamowicz, L., et al. 2007, Astrobiol., 7, 43
 Jetzki, M., Luckhaus, D., & Signorell, R. 2004, Can. J. Chem., 82, 915
 Jørgensen, J. K., Favre, C., Bisschop, S. E., et al. 2012, ApJ, 757, L4
 Marstokk, K. M., & Møllendal, H. 1973, J. Mol. Struct., 16, 259
 Milam, S. N., Savage, C., Brewster, M. A., Ziurys, L. M., et al. 2005, ApJ, 634, 1126
 Pearson, J. C., Müller, H. S. P., Pickett, H. M., Cohen, E. A., & Drouin, B. J. 2010, J. Quant. Spectr. Rad. Transf., 111, 1614
 Pickett, H. M. 1991, J. Mol. Spectrosc., 148, 371
 Senent, M. L. 2004, J. Phys. Chem. A., 108, 6286
 Simakov, A., Sekiguchi, O., Bunkan, A., C., J., & Uggerud, E. 2011, J. Am. Chem. Soc., 133, 20816
 Widicus Weaver, S. L., Butler, R. A. H., Drouin, B. J., et al. 2005, ApJ, 158, 188